Title

Nucleotide and Partner-Protein Control of Bacterial Replicative Helicase Structure and Function

Journal

Molecular Cell, 52(6)

ISSN

1097-2765

Authors

Strycharska, Melania S
Arias-Palomo, Ernesto
Lyubimov, Artem Y
et al.

Publication Date

2013-12-01

DOI

10.1016/j.molcel.2013.11.016

Peer reviewed

Published in final edited form as:
Mol Cell. 2013 December 26; 52(6): 844–854. doi:10.1016/j.molcel.2013.11.016.

Nucleotide and partner-protein control of bacterial replicative helicase structure and function

Melania S. Strycharska[1], **Ernesto Arias-Palomo**[2], **Artem Y. Lyubimov**[3], **Jan P. Erzberger**[5], **Valerie O'Shea**[2], **Carlos J. Bustamante**[1,5,6], and **James M. Berger**[1,5,6,†]

[1]Biophysics Program, University of California, Berkeley, 360 Stanley Hall, Berkeley, CA 94720-3220, USA [2]Department of Biophysics and Biophysical Chemistry, Johns Hopkins University School of Medicine, 725 N. Wolfe Street, WBSB 713, Baltimore, Maryland 21205 [3]Stanford University, Stanford School of Medicine, Clark Center, Room E300, Stanford, CA 94305 [4]ETH Zürich, Institute of Molecular Biology and Biophysics, Schafmattstrasse 20, 8093 Zürich, Switzerland [5]Howard Hughes Medical Institute, University of California, Berkeley, 360 Stanley Hall, Berkeley, CA 94720-3220, USA [6]Department of Molecular and Cell Biology, University of California, Berkeley, 360 Stanley Hall, Berkeley, CA 94720-3220, USA

Abstract

Cellular replication forks are powered by ring-shaped, hexameric helicases that encircle and unwind DNA. To better understand the molecular mechanisms and control of these enzymes, we used multiple methods to investigate the bacterial replicative helicase, DnaB. A 3.3 Å crystal structure of *Aquifex aeolicus* DnaB complexed with nucleotide reveals a new conformational state for this motor protein. Electron microscopy and small angle X-ray scattering studies confirm the state seen crystallographically, showing that the DnaB ATPase domains and an associated N-terminal collar transition between two physical states in a nucleotide-dependent manner. Mutant helicases locked in either collar state are active, but display different capacities to support critical activities such as duplex translocation and primase-dependent RNA synthesis. Our findings establish the DnaB collar as an auto-regulatory hub that controls the ability of the helicase to transition between different functional states in response to nucleotide and both replication initiation and elongation factors.

INTRODUCTION

The accurate and timely replication of DNA is essential for the proliferation of all cells. Dedicated enzymes known as helicases are key drivers of replication fork progression, unwinding parental DNA duplexes to provide single-stranded template to DNA polymerases for strand synthesis (Pomerantz and O'Donnell, 2007). Cellular replicative helicases universally form either homohexameric or heterohexameric rings, which encircle DNA and use ATP hydrolysis to drive the processive separation of paired duplex substrates (Singleton et al., 2007). Despite extensive study, the mechanisms by which hexameric helicases couple

[†]Corresponding author: jmberger@jhmi.edu.

ATP turnover to DNA unwinding remain poorly defined. How helicase activity is coordinated with specific replication initiation and progression factors is likewise unclear.

Replicative hexameric helicases fall into two evolutionarily distinct classes – **M**ini**C**hromosome **M**aintanence (MCM) proteins and DnaB-family enzymes – that share a conserved ATPase fold but that differ in their quaternary organization and accessory domains (Iyer et al., 2004; Leipe et al., 2003; Lyubimov et al., 2011; Wang, 2004). DnaB helicases, which are found in all bacteria, as well as certain bacteriophage (Leipe et al., 2000), assemble into two-tiered homohexameric rings, in which a C-terminal, RecA-type ATPase domain from each of the six subunits comprises one tier and an N-terminal structural domain forms the other (Bailey et al., 2007b; Itsathitphaisarn et al., 2012; Lo et al., 2009; Wang et al., 2008) (Figure 1A). In each DnaB protomer, the N-terminal domain is connected to the C-terminal region by a **L**inker **H**elix (LH) that anchors adjoining subunits together through a domain-swapping event. Interestingly, DnaB-family enzymes all display a natural symmetry mismatch between their two tiers (San Martin et al., 1998; San Martin et al., 1995): the C-terminal domains exhibit variable, but roughly cyclic, quasi-six-fold symmetry (Bailey et al., 2007b; Lo et al., 2009; Wang et al., 2008), whereas the N-terminal domains form homodimers that self-associate into a trimeric collar (Bailey et al., 2007b; Biswas and Tsodikov, 2008; Itsathitphaisarn et al., 2012; Lo et al., 2009; Wang et al., 2008).

Although the C-terminal domains of DnaB are well established as the helicase motor that hydrolyses ATP to power DNA unwinding (Biswas and Biswas, 1999b; Biswas et al., 1994; Leipe et al., 2000; Nakayama et al., 1984), the structural and functional role of the N-terminal collar has been less clear. Some lines of evidence have indicated that the collar, like the motor domains, can bind single-stranded DNA (Bailey et al., 2007b; Lo et al., 2009), as well as serve as a scaffolding element that helps stabilize DnaB hexamers (Biswas et al., 1994) and aid in ring closure (Wang et al., 2008). However, biochemical studies showing that the collar is both important for DNA unwinding and for binding specific partner proteins have hinted at a more complex role for this element in helicase function (Bailey et al., 2007b; Bird et al., 2000; Biswas and Biswas, 1999b; Biswas et al., 1994; Chang and Marians, 2000; Nakayama et al., 1984; Seitz et al., 2000; Xie and He, 2009). For example, the binding of the DnaB collar to DnaG is important for controlling both priming activity and frequency (Johnson et al., 2000; Koepsell et al., 2006; Mitkova et al., 2003; Tougu and Marians, 1996). Conversely, DnaG binding appears to antagonize the association of the helicase with DnaC (Makowska-Grzyska and Kaguni, 2010), an ATP-dependent helicase-loading factor that interacts with the C-terminal face of DnaB opposite the collar (Arias-Palomo et al., 2013; Galletto et al., 2003). Interestingly, whereas DnaG has been shown to engage the collar in a conformation seen in apo crystal structures of DnaB (Bailey et al., 2007b), the collar takes on a markedly different conformation when the helicase associates with nucleotide-bound DnaC. The functional implications of these two collar states for DnaB helicase activity and the factors that lead to their interconversion are not known.

To address questions surrounding the interplay between the structure and function of DnaB, we determined a 3.3 Å resolution X-ray crystal structure of the helicase from *Aquifex aeolicus* in complex with ADP. The structure reveals a hexameric architecture distinct from other previously-observed closed-ring states. In particular, the N-terminal collar has undergone a large conformational rearrangement from that seen in substrate-free helicase structures, transitioning from a widened, or “dilated,” configuration (which encircles a broad central channel), into a highly-constricted form with a narrow pore. Concomitant with this action, the ATP- and nucleic acid-binding elements of DnaB have re-aligned into a new configuration that appears poised to support nucleotide turnover. Using electron microscopy (EM) and small-angle X-ray scattering (SAXS), we confirm that in both *A. aeolicus* and other bacteria, DnaB can adopt the constricted state observed in the crystal structure, and

further demonstrate that this transition is promoted by nucleotide in both the presence and absence of DNA. Structure-derived mutants of *Escherichia coli* DnaB that preferentially form one collar state or the other can unwind DNA, but have markedly altered properties with respect to double-stranded DNA translocation and their ability to support either priming by DnaG or helicase activation by the clamp-loader tau subunit. Together, our data show that, like their eukaryotic counterparts, bacterial replicative helicases are complex, multistate machines whose properties can both modulate and be modulated by other replication factors.

RESULTS AND DISCUSSION

Determination of the A. aeolicus DnaB structure

In the absence of substrate, DnaB-family helicases display a high degree of positional variation and separation in the relative conformations of their C-terminal domains (Bailey et al., 2007b; Lo et al., 2009; Wang et al., 2008). Upon binding of single-stranded DNA and nucleotide, however, the active sites of DnaB have recently been shown to condense into a more uniform, compact conformation that resembles related nucleotide-bound, hexameric helicases such as the Rho transcription termination factor and T7 bacteriophage gp4 (Itsathitphaisarn et al., 2012; Singleton et al., 2000; Thomsen and Berger, 2009). Interestingly, EM experiments have indicated that conformational heterogeneity persists within DnaB even when nucleotide is present, implying that the fully-liganded helicase still exhibits significant plasticity (Yang et al., 2002; Yu et al., 1996).

To better define the physical consequences of nucleotide binding to DnaB, we determined the crystal structure of the full-length helicase from *A. aeolicus*. The primary sequence of *Aa*DnaB is 40% identical to related enzymes in its family (Figure S1). Crystals of the protein diffracted to 3.3 Å resolution and belonged to the cubic spacegroup $I2_13$. Solution of the structure by molecular replacement revealed one DnaB homodimer per asymmetric unit, with the operation of a crystallographic three-fold symmetry generating a two-tiered, hexameric particle formed by a set of N-terminal scaffolding elements (tier 1) and a set of C-terminal ATPase domains (tier 2) (Figure 1B). Electron density maps showed clear evidence for ADP•Mg^{2+} bound at each interface between adjacent monomers (Figure 1C). The final model was refined to an R_{work}/R_{free} of 22.1%/25.9%, with excellent stereochemistry as judged by MolProbity (Chen et al., 2010) (Table 1).

To ascertain whether the crystal structure we determined corresponded to a native state of *Aa*DnaB, we turned to negative-stain EM (Figure S2). The resultant 23 Å resolution EM reconstruction proved highly similar to the atomic structure, as judged by the close resemblance of EM model reprojections with projections calculated from both the crystal structure and reference-free, experimental 2D class averages (Figure 1D). The close similarity is readily apparent upon fitting of the atomic coordinates into the EM reconstruction (CC=0.87; Figure 1E). Together, these data demonstrate that the conformation of *Aa*DnaB found in the crystal corresponds to a dominant population state of the protein in general.

Nucleotide binding promotes ATPase domain engagement and a novel conformation of the N-terminal collar

Within the *Aa*DnaB hexamer, all six ATPase domains interact extensively with each other (~1000$Å^2$ per protomer), forming a pseudo-6-fold symmetric (trimer-of-dimers) ring with a narrow central pore. Although the ADP molecules bound in the active site lack a γ-PO_4, an invariant arginine donated *in trans* from each subunit into its neighboring protomer's active site (the "arg-finger"), assumes a configuration approximating that seen in catalytically-

competent nucleotide-binding sites of related RecA ATPases in general (Figure S3A-C). Interestingly, the base and sugar of each nucleotide is bound non-canonically by *Aa*DnaB compared to other RecA systems such as T7 gp4 and Rho; in particular, a hydrophobic binding pocket that normally ligands the purine or pyrimidine moiety of an NTP has collapsed, causing the base to flip into an inter-subunit cleft (Figure S3B-D). Inspection of a recent GDP•AlF4-associated DnaB structure reveals a similar binding mechanism to that seen for *Aa*DnaB (Figure S3D), suggesting that bacterial replicative helicases have evolved a divergent means for coordinating substrate nucleotides within the RecA ATPase superfamily.

A distinguishing feature of all bacterial (and certain phage) DnaB-family helicases from other RecA-family ring ATPases is the presence of a conserved N-terminal domain consisting of a globular helical bundle appended to an extended α-helical hairpin (Bailey et al., 2007a, b; Fass et al., 1999; Itsathitphaisarn et al., 2012; Kashav et al., 2009; Lo et al., 2009; Wang et al., 2008; Weigelt et al., 1999). The helical hairpins of two neighboring N-terminal domains form homodimers, giving rise to a twin-lobed, dumbbell-shaped element. Both on their own and in the context of a DnaB hexamer, neighboring N-terminal domain dimers have been seen to self-organize into a triangular, trimeric structure that circumscribes a wide inner channel (~50Å in diameter) (Figure 2A) (Bailey et al., 2007b; Biswas and Tsodikov, 2008; Itsathitphaisarn et al., 2012; Lo et al., 2009; Wang et al., 2008). The sides of the triangle are formed by helical hairpin dimers of the N-terminal domains, whereas the apices are created by globular helical bundles from different dimers that abut one another. Thus far, only one type of trimer configuration has been observed for the N-terminal collar in the context of DnaB alone, indicating it is a favored quaternary state of the region.

The conformation seen for the *Aa*DnaB N-terminal domains differs markedly in comparison to other DnaB structures (Figure 2A). Although the N-terminal domains of the helicase maintain the hairpin interfaces within each homodimer, the globular domains of adjoining dimers manifest a completely different set of interactions between each other (Figure 2A, S3E). In attaining this state, each N-terminal homodimer has undergone an ~40° rotation within the plane of the ring, projecting three globular lobes outward from the ring and clustering three others in the interior (Movie S1). The resultant rearrangement leads to a distinctive triskelion that constricts the diameter of the channel formed between the N-terminal domains by ~30 Å from that seen in the other, more dilated state (Figure 2A). The new interactions between the globular subdomains and the distal ends of the helical hairpins are modest, reducing the buried surface area per globular subdomain by ~40% compared to the widened, triangular form (from 370$Å^2$ to 230 $Å^2$) (Figure S3E).

At first glance, constriction of the N-terminal domains would appear to help promote the observed tightening of the C-terminal domains and formation of productive ATPase centers. However, close engagement of neighboring motor domains is also seen in the structure of *G. stearothermophilus* DnaB bound to ssDNA and nucleotide, which exhibits a dilated collar. A significant structural difference between these two states is that the *Gst*DnaB hexamer forms a lockwasher, or cracked-spiral configuration, whereas the *Aa*DnaB ring is closed-planar. However, in both instances, ATPase domain clustering is coincident with an inward tilt toward the pore of the ring compared to that seen in apo DnaB models (Figure 2B-C). Tilting appears to be coordinated by both a linker α-helix that connects the N- and C-terminal domains together and by an additional α-helix in the motor domains. This latter α-helix in particular makes extensive contacts with the N-terminal domain of a neighboring protomer when the collar is dilated, but with its own N-terminal domain upon entry into the constricted state, suggesting that it helps to transduce conformational signals between the two domains (Movie S2). Consistent with this notion, mutations in the transducer helix have pronounced effects on properties such as single-stranded DNA binding, the DNA-

dependence of ATP hydrolysis, and DNA unwinding (Biswas and Biswas, 1999a, b; Nitharwal et al., 2012).

Nucleotide alters the conformational equilibrium between dilated and constricted states

Because the constricted *Aa*DnaB state had not been observed previously, we set out to determine whether it was specific to the thermophilic protein, and whether nucleotide might help promote constriction. Using the well-studied *E. coli* DnaB helicase as a model system, we prepared samples both in the presence and absence of ATP and the ATP analogs AMPPNP, ADP•BeF_3 and ATPγS, and analyzed these complexes by EM. 2D classification of apo *Ec*DnaB failed to reveal any evidence for a constricted particle state, showing only dilated forms of the enzyme (Figure 3A). By contrast, two kinds of 2D class averages were observed for *Ec*DnaB in the presence of ATPγS, ATP and AMPPNP (Figure 3A, Figure S4A), approximately half of which adopted a dilated configuration and the other half a constricted state. These findings demonstrate that while a dilated ring conformation is the default state for *E*cDnaB, nucleotide can trigger the enzyme to switch into a constricted form (Figure 3A).

To better define the factors controlling the dilated/constricted transition, we next used EM to look at the distribution of the two *Ec*DnaB states under different substrate-binding conditions. Interestingly, even at nucleotide concentrations as high as 5mM, 2D class averages showed that *Ec*DnaB did not fully shift to the constricted state. The inclusion of ssDNA (ranging from 10 to 35 bases in length) and nucleotide in the sample likewise did not appear to have any additional effect on the distribution of the two populations (although the classes did show extra density inside the helicase pore, consistent with DNA binding Figure S4B). Single-stranded DNA alone was unable to induce any apparent ring constriction. As an additional comparison, we examined the nucleotide-dependent response of *Gst*DnaB, whose crystal structures have thus far exhibited only dilated forms of the protein (Bailey et al., 2007b; Itsathitphaisarn et al., 2012); 2D EM analysis again revealed evidence for a constricted species in the presence of ATP (Figure S4C). Together, these findings show that the nucleotide-dependent constriction seen for *Aa*DnaB is conserved across different DnaB homologs, but that ATP does not appear capable of completely transforming an entire population of DnaB particles from one state to another.

Specific intersubunit interactions mediate the stability of the N-terminal collar

The inability of closed-ring *Ec*DnaB hexamers to fully transition from a dilated to constricted state upon binding nucleotide was somewhat unexpected. On the one hand, this behavior could reflect the existence of inactive particles in our sample preparations, which might have failed to interconvert because of a local assembly defect or due to an inability to properly bind ATP. Alternatively, the interactions between N-terminal domain homodimers might be sufficiently strong that nucleotide binding can only provide a portion of energy necessary to overcome the free energy barrier of their association in the dilated state, thereby predisposing DnaB to oscillate between the two forms in solution.

To distinguish between these possibilities, we created point mutations in *Ec*DnaB that would be expected to disrupt or stabilize interfaces present in the dilated form of the N-terminal collar ring, and used 2D EM to observe the conformations accessible to our mutants. Since no crystal structures of full-length *Ec*DnaB are currently available, we created homology models for the *E. coli* helicase using *Gst*DnaB and *Aa*DnaB as templates. This analysis identified two sidechains, Ser36 and Ile85, which are closely apposed in the dilated collar interface of DnaB but solvent-exposed in the constricted form (Figure 3B, S5A). Both residues were replaced with arginines to generate electrostatic repulsion between the globular heads in the dilated ring state and favor ring constriction. We next replaced Thr86

and Ala121, which lie ~5 Å apart in the dilated state, with cysteines to create a second *Ec*DnaB mutant that could be prevented from assuming a constricted collar conformation via disulfide bonds (Figure 3B, S5B,C). Consistent with our predictions, 2D class averages revealed that the S36R/I85R mutant exclusively adopted a constricted conformation (Figure 3A), whereas the oxidized T86C/A121C construct formed only dilated species even in the presence of 1mM ATP (Figure 3A). Together, these findings demonstrate that inter-subunit contacts between the N-terminal domains not only help control the conformational state of DnaB, but that these elements also predispose the native helicase toward a dilated configuration.

To further check that the DnaB conformations seen crystallographically and by EM correspond to solution states when nucleotide is present, we turned to small-angle X-ray scattering (SAXS). Theoretical calculation of scattering curves using homology models of the *E. coli* helicase threaded onto either the ADP-bound (constricted) *Aa*DnaB structure, or the fully-liganded (dilated) *Gst*DnaB coordinates, revealed distinct SAXS signatures for the two conformations; in particular, a distinguishing dip and hump, visible from q=0.07-0.1 for the dilated state, flattens out in the constricted form (Figure 3C). Consistent with this difference, SAXS analysis of our dilated and constricted *Ec*DnaB mutants revealed profiles respectively similar to the two extremes. Moreover, data obtained for wild-type *Ec*DnaB in the presence of nucleotide showed an intermediate hump, suggestive of a mixture of the two states. Collectively, these observations indicate that DnaB collar can adopt at least two highly-distinct conformations, and that nucleotide can toggle a switch from one form to the other.

Ring constriction and dilation aids in distinguishing between single and double stranded DNA substrates

Although our structural data highlighted the existence of a two-state collar transition in DnaB, the functional significance of the dilated and constricted forms was not immediately apparent. We therefore set out to assess the consequences of the two states on DnaB activity, using our mutants to bias the helicase into one collar state or the other. When assessed for single-stranded DNA binding using fluorescence anisotropy, with substrates ranging from 15 to 60 nulceotides in length, the constricted and dilated *Ec*DnaB mutants both showed a similar affinity compared to the wild-type enzyme (Figure 4A). However, when double-stranded DNA substrates long enough to span the full length of the central channel were investigated, the dilated mutant showed a >2-fold increase in binding affinity relative to the wild type protein, whereas the constricted conformation displayed a >2-fold decrease (K_Ds of 28nM, 70nM and 180nM respectively, Figure 4B). These results indicate that both conformations of DnaB helicase can accommodate single DNA strands equally well inside the helicase pore, but that the constricted conformation of the helicase is less able to engage duplex substrates.

We next compared the basal, as well as single- and double-stranded DNA stimulated, ATP hydrolysis rates of the mutant and wild type proteins, utilizing a coupled enzyme assay and DNA substrates identical to those used in the DNA-binding experiments. The constricted mutant and wild-type DnaB helicase had very similar basal hydrolysis rates that were both greatly stimulated by the addition of single-stranded DNA (Figure 4C). In agreement with its reduced affinity for double-stranded DNA, the constricted conformation showed negligible stimulation of hydrolysis by duplex oligos (Figure 4D). By contrast, the dilated mutant displayed basal hydrolysis rates equivalent to the DNA-stimulated rates of wild type and constricted DnaB. Moreover, these rates were relatively unaffected by the addition of DNA (Figure 4C-D), indicating that stabilization of the N-terminal collar in a dilated state uncoupled ATPase activity from DNA binding. Interestingly, a similar decoupling has been

observed when mutations have been introduced into the DnaB **T**ransducer **H**elix (TH) that forms the interface between the N-terminal collar and the C-terminal ATPase ring (Biswas and Biswas, 1999a).

To further understand the functional impact of a change in DnaB collar state, we measured the ability of both mutant and wild type DnaBs to translocate along dsDNA substrates; although DnaB is thought to move along a single-DNA strand when acting as a helicase (Jezewska et al., 1998; Kaplan and Steitz, 1999; LeBowitz and McMacken, 1986), it also can drive the powered movement of DNA duplexes (Kaplan, 2000; Kaplan and O'Donnell, 2002). Using a fluorescent assay outlined in Figure 4E, we found that whereas wild-type and dilated DnaB helicases were able to translocate along double-stranded DNA, the constricted mutant could not (Figure 4F, S6). Taken together with our DNA-binding and ATP-hydrolysis data, these observations not only reveal that the structural disposition of the N-terminal collar directly helps coordinate nucleotide turnover with DNA binding, but also show that changes in collar state can control whether DnaB can translocate along dsDNA, likely by sterically preventing duplex DNA entry into the motor when the collar is constricted.

As a final assessment of the effects of collar state on internal DnaB functions, we next looked at the unwinding of duplex DNA by the helicase. On short model duplexes, DnaB family enzymes are most active when one oligonucleotide end bears a single-stranded fork (Figure S6C) (Kaplan, 2000; Kaplan and Steitz, 1999); *E. coli* DnaC, a helicase loader, further stimulates the action of its cognate DnaB on these substrates (Arias-Palomo et al., 2013). As seen previously (Arias-Palomo et al., 2013), wild-type DnaB displayed relatively little unwinding activity in the absence of the helicase loader (Figure 5A). The behavior of dilated mutant largely mirrored that of the native enzyme; however, the constricted mutant actually showed a moderately elevated degree of basal unwinding (Figure 5A), indicating that this construct is not an inherently crippled motor. When the dilated and constricted mutants were tested in a single-turnover, fork-unwinding assay with DnaC, the dilated mutant was able to produce ~20% more unwound product as the wild type helicase, and did so at a slightly faster rate (Figure 5B). By contrast, while the constricted mutant could generate a comparable amount of single-stranded DNA as wild-type DnaB, it took longer to do so (Figure 5B).

Together, our DNA unwinding data indicate that, unlike with double-stranded DNA translocation, DnaB can function as a helicase regardless of whether its collar is dilated or constricted. However, the observed differences in the rates at which the mutants promote product formation show that the collar can have an unexpectedly profound effect on the kinetics of helicase action. Interestingly, *Gst*DnaB has been seen to form a cracked, but dilated, N-terminal collar conformation when bound both to nucleotide and to a single-stranded DNA substrate proposed to reflect a translocation substrate (Itsathitphaisarn et al., 2012). This structural finding suggests that the elevated unwinding rates seen with a dilated collar could result from an ability of the mutant helicase to more stably retain a translocation-competent configuration. If true, then the moderate pace of the wild-type enzyme might result from continuous interconversion between this state and a slower moving form, one our data suggest could derive from a constricted collar configuration. Alternatively, 3D EM reconstructions of an *Ec*DnaB•DnaC complex have shown that upon binding of DnaC, contacts between the globular domains of the DnaB N-terminal collar rearrange into a cracked , but constricted, configuration (Arias-Palomo et al., 2013). Given that DnaC is present in our unwinding assays, and that the loader is known to prevent DnaB from unwinding DNA when it stays associated with the helicase (Biswas et al., 1986; Wahle et al., 1989), the observed differences in rate between wild-type and mutant DnaBs seen here could derive from a change in the relative affinity of DnaC for the helicase depending on the

state of the collar. In this view, a constricted collar state would favor DnaC binding, slowing release of the loader from the helicase and leading to a long lag that precedes unwinding. By contrast, a dilated collar would disfavor interactions with DnaC, speeding loader release to relieve inhibition of the helicase and promote more rapid unwinding. Future efforts will be needed to distinguish between these possibilities.

Differential interaction and response of constricted and dilated DnaB conformers with replisomal partner proteins

Intrigued by the possibility that DnaB might use different conformations of its collar to modulate its own activity and/or the binding propensity of DnaC, we set out to investigate whether changes in collar state might affect interactions between the helicase and some of its other partner proteins. One such factor is the τ subunit of the DNA polymerase clamp loader (Dallmann et al., 2000; Kim et al., 1996). As with DnaC, *E. coli* τ has been reported to bind to the C-terminal motor domains of DnaB (Haroniti et al., 2004; Martinez-Jimenez et al., 2002); mass-spectrometry studies have further found that domains III and IV of τ associate more strongly with DnaB in the presence of ATP and Mg^{2+} (Afonso et al., 2013), conditions shown here to promote collar constriction. To test whether τ could distinguish between different N-terminal domain conformations of DnaB, we examined the effect of its helicase-binding domains on DNA unwinding by the *E. coli* helicase. Notably, the presence of τ domains III-IV stimulated strand separation by all DnaB constructs tested. However, the highest degree of stimulation was actually exhibited by the constricted DnaB mutant, with levels approaching those seen for the dilated DnaB mutant when activated by DnaC (compare Figures 5B and 5C). Thus, as with DnaC, τ also appears capable of distinguishing between different DnaB collar states. How τ reads out the collar confirmation of DnaB is not clear: the protein could recognize a cryptic binding site on the N-terminal domains that is revealed upon collar constriction, or movements in the collar might allosterically remodel the existing τ binding site in DnaB's C-terminal motor region to favor more productive interactions.

A second replisomal factor that binds to DnaB is the DnaG primase (Bailey et al., 2007b; Bird et al., 2000; Chang and Marians, 2000). In a co-crystal structure of *Gst*DnaB bound to the C-terminus of DnaG (Bailey et al., 2007b), the helicase-interaction domain of primase, which is itself a structural homolog of the DnaB N-terminal domain (Chintakayala et al., 2007; Oakley et al., 2005; Syson et al., 2005), can be seen to bind non-equivalently to two adjacent, but distinct, globular heads of a dilated DnaB collar (Figure S7A). Interestingly, the disposition of DnaG-binding sites is dramatically different in the constricted state, with one site rendered sterically inaccessible and the other repositioned far from the central pore of the helicase (Figure S7B).

The change in DnaG-binding site configurations between the two collar states immediately suggested that DnaG might preferentially associate with DnaB when the helicase collar is dilated compared to when it is constricted. To test this idea, we assessed the ability of different DnaB collar mutants to stimulate primer synthesis by DnaG, a well-characterized activity that can be monitored in an M13 priming assay by titrating different amounts of helicase against a fixed concentration of primase (Johnson et al., 2000; Koepsell et al., 2005; Lu et al., 1996). Notably, we observed that while the dilated mutant enhanced primer synthesis to the same degree as wild-type *Ec*DnaB, the constricted helicase was completely unable to stimulate DnaG activity (Figure 5D). These findings not only corroborate prior structural data showing that primase associates with a dilated form of the DnaB N-terminal domains (Bailey et al., 2007b), but also demonstrate that the conformational state of the collar can directly control the efficiency of primer formation.

The N-terminal collar is a control locus for regulating DnaB structure and function

All bacteria rely on a DnaB family helicase for DNA replication (Ilyina et al., 1992; Leipe et al., 2000). Although the translocation and unwinding activity of the DnaB C-terminal domains is well appreciated (Bird et al., 2000; Biswas and Biswas, 1999b; Nakayama et al., 1984), the function of the DnaB N-terminal collar has remained enigmatic. To date, the collar has been shown both to stabilize DnaB hexamers (Biswas et al., 1994) and to sterically impede aberrant loading onto DNA (Arias-Palomo et al., 2013). Whether the N-terminal domains might play a more fundamental part of DnaB function other than as a basic scaffolding element has been unresolved.

The structural and mutagenesis data presented here establish a new and unexpected role for the N-terminal collar as a nucleotide-actuated locus for controlling DnaB conformation. Our data further show that these states can regulate both intrinsic helicase functions, such as double-stranded DNA translocation, and the interplay between DnaB and its associated replication factors. Consideration of these data in light of the known activities of DnaB reveals a rich pattern by which structural interconversions in the helicase could be used to help direct a myriad number of replication-dependent processes (Figure 6). For example, a dilated form of the collar not only supports DnaG-dependent priming (Figure 5D), but also appears to help repress helicase activity in the absence of any binding partners (possibly as a means to prevent inopportune replication onset) (Figure 5A). By comparison, when constricted, the collar appears to favor interactions with DnaC (Arias-Palomo et al., 2013), likely to promote loading onto replication origins during initiation, and is uniquely responsive to τ (Figure 5C), a property that may aid with clamp loader recruitment during fork progression. Consistent with these notions, the association of DnaG with DnaB has been shown to help displace DnaC from the helicase during initiation (Makowska-Grzyska and Kaguni, 2010). We posit that this activity likely derives from an ability of primase to stabilize a dilated collar conformation that allosterically antagonizes DnaC binding to DnaB, and that DnaG and τ might similarly alter the relative binding of each other by promoting the formation of different helicase states.

A second unanticipated outcome of this work is the finding that while both DnaB collar states can support helicase activity (Figures 5B and 5C), and hence translocation along single-stranded DNA, only helicases that can access a dilated state can move along double-stranded DNA (Figure 4F). This observation indicates that the dilated conformation recently seen for *Gst*DnaB when bound to single-stranded DNA and nucleotide (Itsathitphaisarn et al., 2012) may also be accessed by the helicase when binding duplex substrates (Figure S7C). Interestingly, dilated and constricted DnaB mutants also appear to differ in their relative rates of unwinding. Although this difference (which is most apparent in reactions that rely on DnaC to promote unwinding) may derive from a preference of the loader for one state over another, it is possible that constricted and dilated forms could also translocate along DNA at different rates. Additional studies will be required to test these concepts.

Concluding remarks

The work described here reveals the existence of a new structural configuration and ATP-responsive autoregulatory locus in bacterial DnaB-family helicases. Coupled with biochemical analyses, these findings not only provide unanticipated insights into the molecular action of DnaB, but also demonstrate that the structural and functional responses of DnaB to its substrates and partner proteins are more varied and nuanced than previously established. In particular, the enzyme can interconvert between at least two distinct global conformations, each of which exhibits distinct biochemical properties that could be exploited differentially to support and regulate alternate replication events such as initiation and elongation. This complexity highlights an unexpected, but convergently evolved,

parallel between the replicative helicases of bacteria and eukaryotes, whereby the MCM2-7 helicase also accesses multiple conformational and functional states in a manner controlled by different types of regulatory factors (Brewster and Chen, 2010; Costa et al., 2013; Remus and Diffley, 2009).

EXPERIMENTAL PROCEDURES

(Details for all experimental methods can be found in Extended Experimental Procedures.)

Protein expression and purification

*Aa*DnaB was expressed in *E. coli* from a pET-28b derived plasmid. Following harvesting and lysis, protein was purified by heat-treatment and column chromatography (ion exchange and gel filtration). Fresh protein was used for crystallography, while small aliquots were stored at −80°C for subsequent EM studies. *Ec*DnaB and DnaC were purified according to the protocols in (Arias-Palomo et al., 2013). Because of toxicity, the constricted double-arginine mutant of *Ec*DnaB was cloned into a periplasmic expression vector with a N-terminal affinity tag, expressed, and purified by column chromatography (Ni^{2+}, ion exchange and gel filtration). The dilated *Ec*DnaB mutant was initially purified as the wild type protein. Following the first gel filtration column, the sample was dialyzed out of nucleotide and reducing agent and run over the second gel filtration column in the absence of nucleotide and DTT to promote cross-linking. *Gst*DnaB was expressed with an N-terminal affinity tag and purified by column chromatography (Ni^{2+}, ion exchange and gel filtration). *Ec*DnaG protein was obtained from Richard Rymer (Berger Laboratory) and τ domains III and IV were obtained from Tiago Barros (Kuriyan Laboratory).

Structural methods

For crystallization, *Aa*DnaB was dialyzed overnight into 10mM HEPES pH 7.5, 50mM KCl, 5mM $MgCl_2$, 1mM ADP, and 0.1mM AMPPNP. Hanging-drop crystals were grown over well solution containing 100mM Hepes pH 7.5, 200-300mM KSCN or NaSCN and 18-22% PEG 3350. For cryoprotection, crystals were harvested into well solution plus 25% MPD, looped and plunged into liquid nitrogen; x-ray Diffraction data were collected on Beamline 8.3.1 at the Advanced Light Source. For EM analysis, *Aa*DnaB, *Ec*DnaB and *Gst*DnaB samples were dialyzed over night and run over an analytical sizing column prior to each EM experiment. Samples were deposited onto grids and stained with 2% (w/v) uranyl formate, after which data were collected on Tecnai 12 BIOTWIN (FEI) at 120 kV using a Temcam-f416 CMOS detector (TVIPS). For SAXS, data were collected at beamline BL4-2 of the Stanford Synchrotron Radiation Lightsource. The samples contained 1 mg/mL wild type and mutant *Ec*DnaB (dialyzed out of nucleotide overnight and run over an analytical sizing column prior to data collection), with the inclusion of nucleotide in 3-fold dilution steps from 0 mM to 1 mM AMPPNP. Details on crystallographic, EM and SAXS data processing, modeling, etc. can be found in Extended Experimental Methods.

Accession codes

The *Aa*DnaB x-ray model was deposited into the RCSB PDB (ID: 4NMN) and the *Aa*DnaB 3D EM reconstruction into the EMDB (ID: EMD-2508).

Biochemistry

DNA binding, ATP hydrolysis, fork unwinding and dsDNA translocation assays were performed in a buffer containing 20 mM HEPES-KOH pH 7.5, 5 mM magnesium acetate, 50 mM potassium glutamate, 5 % glycerol and 0.2 mg/mL BSA. DNA binding experiments were done in 0.5 mM AMPPNP, and unwinding and translocation assay in 1mM ATP.

Primer synthesis data was collected in 100mM potassium glutamate, 20mM HEPES-KOH pH 7.5, 10mM magnesium acetate and 0.2mg/ml BSA. All biochemical characterization was done in the absence of reducing reagents to ensure efficient disulfide bond formation of the cross-linked dilated DnaB mutant. DNA binding reactions contained 10nM DNA labeled with fluorescein at 5' end (the duplex DNA substrate had only one labeled strand). Protein was titrated into the binding reactions in concentrations ranging from 0-1 μM hexamer (for single-stranded DNA binding) or 0-4 μM hexamer (for duplex DNA binding). Binding assays were performed in triplicate and the average anisotropy value plotted as a function of DnaB hexamer concentration. Binding curves were fit to a simple, single-site with Hill slope binding equation using PRISM (GraphPad).

ATPase assay

Wild type and mutant ATPase activities were measured using an established enzyme-coupled assay in which the hydrolysis of ATP to ADP is coupled to the oxidation of NADH to NAD+ (Tamura and Gellert, 1990). To determine Km and V_{max}, 25 nM of DnaB hexamer was incubated at 37° C with 0-1.6 mM ATP in 100 μL reactions. ATPase rate as a function of ATP concentration was fit using Michaelis-Menten kinetics in PRISM (GraphPad). DNA stimulation of ATPase activity was measured by addition of 500 nM unlabeled ss/dsDNA substrates used in DNA binding assays. Reported values are an average of four measurements.

dsDNA translocation and fork unwinding

Measurements of DNA unwinding were carried out as previously described (Arias-Palomo et al., 2013). Measurements are reported as an average of six reactions. DNA substrates used are shown in Figure S6A.

Primer Synthesis Assay

Primer synthesis assays, performed in triplicate, were based on previously described methods (Koepsell et al., 2005). All reactions were carried out in 30 μl volume containing 0.2mM each of ATP, UTP, GTP and CTP, 3.3 nM ssM13 DNA (New England Biolabs) ,and 500nM DnaG. Preincubated Dna(BC)6 complex was included at concentrations ranging from 0 to 1.5 μM. Primase was mixed with $Dna(BC)_6$ for 1 min at 37° C, then NTPs were added together with ssM13 DNA and the mixture incubated for additional 5 min. Reactions were stopped by addition of 30 μL of 1:100 PicoGreen stock solution (Invitrogen) in 20mM Tris-HCl plus 50mM EDTA (pH 7.5). Stopped reactions were incubated in the dark for 5min and raw fluorescence was measured in a Victor ^{3}V plate reader (Perking Elmer).

Supplementary Material

Refer to Web version on PubMed Central for supplementary material.

Acknowledgments

The authors are grateful to the Nogales laboratory and the staff at beamlines 8.3.1 and 12.3.1 of the Advanced Light Source and beamline BL4-2 of the Stanford Synchrotron Radiation Lightsource for help with data collection and analysis, and to the Berger laboratory for helpful discussions and aid in preparing the manuscript. We also thank Richard Rymer for providing DnaG protein, Seychelle Vos for help collecting SAXS data, Gregory Hura for help with processing SAXS data, and Tiago Barros of the Kuriyan lab for the τ domains III and IV construct. This work was supported by the Programa Nacional de Movilidad de Recursos Humanos del Plan Nacional de I-D+i 2008-2011 from the Spanish Ministry of Education to EAP, an American Cancer Soceity post-doctoral fellowship to AYL, and the NIGMS (to JMB, RO1-GM071747).

REFERENCES

Afonso JP, Chintakayala K, Suwannachart C, Sedelnikova S, Giles K, Hoyes JB, Soultanas P, Rafferty JB, Oldham NJ. Insights into the structure and assembly of the Bacillus subtilis clamp-loader complex and its interaction with the replicative helicase. Nucleic Acids Res. 2013; 41:5115–5126. [PubMed: 23525462]

Arias-Palomo E, O'Shea VL, Hood IV, Berger JM. The bacterial DnaC helicase loader is a DnaB ring breaker. Cell. 2013; 153:438–448. [PubMed: 23562643]

Bailey S, Eliason WK, Steitz TA. The crystal structure of the Thermus aquaticus DnaB helicase monomer. Nucleic Acids Res. 2007a; 35:4728–4736. [PubMed: 17606462]

Bailey S, Eliason WK, Steitz TA. Structure of hexameric DnaB helicase and its complex with a domain of DnaG primase. Science. 2007b; 318:459–463. [PubMed: 17947583]

Bird LE, Pan H, Soultanas P, Wigley DB. Mapping protein-protein interactions within a stable complex of DNA primase and DnaB helicase from Bacillus stearothermophilus. Biochemistry. 2000; 39:171–182. [PubMed: 10625492]

Biswas EE, Biswas SB. Mechanism of DNA binding by the DnaB helicase of Escherichia coli: analysis of the roles of domain gamma in DNA binding. Biochemistry. 1999a; 38:10929–10939. [PubMed: 10460148]

Biswas EE, Biswas SB. Mechanism of DnaB helicase of Escherichia coli: structural domains involved in ATP hydrolysis, DNA binding, and oligomerization. Biochemistry. 1999b; 38:10919–10928. [PubMed: 10460147]

Biswas EE, Biswas SB, Bishop JE. The dnaB protein of Escherichia coli: mechanism of nucleotide binding, hydrolysis, and modulation by dnaC protein. Biochemistry. 1986; 25:7368–7374. [PubMed: 3026453]

Biswas SB, Chen PH, Biswas EE. Structure and function of Escherichia coli DnaB protein: role of the N-terminal domain in helicase activity. Biochemistry. 1994; 33:11307–11314. [PubMed: 7727381]

Biswas T, Tsodikov OV. Hexameric ring structure of the N-terminal domain of Mycobacterium tuberculosis DnaB helicase. FEBS J. 2008; 275:3064–3071. [PubMed: 18479467]

Brewster AS, Chen XS. Insights into the MCM functional mechanism: lessons learned from the archaeal MCM complex. Crit Rev Biochem Mol Biol. 2010; 45:243–256. [PubMed: 20441442]

Chang P, Marians KJ. Identification of a region of Escherichia coli DnaB required for functional interaction with DnaG at the replication fork. J Biol Chem. 2000; 275:26187–26195. [PubMed: 10833513]

Chen VB, Arendall WB, Headd JJ, Keedy DA, Immormino RM, Kapral GJ, Murray LW, Richardson JS, Richardson DC. MolProbity: all-atom structure validation for macromolecular crystallography. Acta Crystallogr D Biol Crystallogr (3rd). 2010; 66:12–21. [PubMed: 20057044]

Chintakayala K, Larson MA, Grainger WH, Scott DJ, Griep MA, Hinrichs SH, Soultanas P. Domain swapping reveals that the C- and N- terminal domains of DnaG and DnaB, respectively, are functional homologues. Mol Microbiol. 2007; 63:1629–1639. [PubMed: 17367384]

Costa A, Hood IV, Berger JM. Mechanisms for Initiating Cellular DNA Replication. Annual Review of Biochemistry. 2013; 82:25. Vol 82.

Dallmann HG, Kim S, Pritchard AE, Marians KJ, McHenry CS. Characterization of the unique C terminus of the Escherichia coli tau DnaX protein. Monomeric C-tau binds alpha AND DnaB and can partially replace tau in reconstituted replication forks. J Biol Chem. 2000; 275:15512–15519. [PubMed: 10748120]

Fass D, Bogden CE, Berger JM. Crystal structure of the N-terminal domain of the DnaB hexameric helicase. Structure. 1999; 7:691–698. [PubMed: 10404598]

Galletto R, Jezewska MJ, Bujalowski W. Interactions of the Escherichia coli DnaB helicase hexamer with the replication factor the DnaC protein. Effect of nucleotide cofactors and the ssDNA on protein-protein interactions and the topology of the complex. J Mol Biol. 2003; 329:441–465. [PubMed: 12767828]

Haroniti A, Anderson C, Doddridge Z, Gardiner L, Roberts CJ, Allen S, Soultanas P. The clamp-loader-helicase interaction in Bacillus. Atomic force microscopy reveals the structural organisation of the DnaB-tau complex in Bacillus. J Mol Biol. 2004; 336:381–393. [PubMed: 14757052]

Ilyina TV, Gorbalenya AE, Koonin EV. Organization and evolution of bacterial and bacteriophage primase-helicase systems. J Mol Evol. 1992; 34:351–357. [PubMed: 1569588]

Itsathitphaisarn O, Wing RA, Eliason WK, Wang J, Steitz TA. The hexameric helicase DnaB adopts a nonplanar conformation during translocation. Cell. 2012; 151:267–277. [PubMed: 23022319]

Iyer LM, Leipe DD, Koonin EV, Aravind L. Evolutionary history and higher order classification of AAA+ ATPases. J Struct Biol. 2004; 146:11–31. [PubMed: 15037234]

Jezewska MJ, Rajendran S, Bujalowska D, Bujalowski W. Does single-stranded DNA pass through the inner channel of the protein hexamer in the complex with the Escherichia coli DnaB Helicase? Fluorescence energy transfer studies. J Biol Chem. 1998; 273:10515–10529. [PubMed: 9553111]

Johnson SK, Bhattacharyya S, Griep MA. DnaB helicase stimulates primer synthesis activity on short oligonucleotide templates. Biochemistry. 2000; 39:736–744. [PubMed: 10651639]

Kaplan DL. The 3'-tail of a forked-duplex sterically determines whether one or two DNA strands pass through the central channel of a replication-fork helicase. J Mol Biol. 2000; 301:285–299. [PubMed: 10926510]

Kaplan DL, O'Donnell M. DnaB drives DNA branch migration and dislodges proteins while encircling two DNA strands. Mol Cell. 2002; 10:647–657. [PubMed: 12408831]

Kaplan DL, Steitz TA. DnaB from Thermus aquaticus unwinds forked duplex DNA with an asymmetric tail length dependence. J Biol Chem. 1999; 274:6889–6897. [PubMed: 10066742]

Kashav T, Nitharwal R, Abdulrehman SA, Gabdoulkhakov A, Saenger W, Dhar SK, Gourinath S. Three-dimensional structure of N-terminal domain of DnaB helicase and helicase-primase interactions in Helicobacter pylori. PLoS One. 2009; 4:e7515. [PubMed: 19841750]

Kim S, Dallmann HG, McHenry CS, Marians KJ. Coupling of a replicative polymerase and helicase: a tau-DnaB interaction mediates rapid replication fork movement. Cell. 1996; 84:643–650. [PubMed: 8598050]

Koepsell SA, Hanson S, Hinrichs SH, Griep MA. Fluorometric assay for bacterial primases. Anal Biochem. 2005; 339:353–355. [PubMed: 15797579]

Koepsell SA, Larson MA, Griep MA, Hinrichs SH. Staphylococcus aureus helicase but not Escherichia coli helicase stimulates S. aureus primase activity and maintains initiation specificity. J Bacteriol. 2006; 188:4673–4680. [PubMed: 16788176]

LeBowitz JH, McMacken R. The Escherichia coli dnaB replication protein is a DNA helicase. J Biol Chem. 1986; 261:4738–4748. [PubMed: 3007474]

Leipe DD, Aravind L, Grishin NV, Koonin EV. The bacterial replicative helicase DnaB evolved from a RecA duplication. Genome Res. 2000; 10:5–16. [PubMed: 10645945]

Leipe DD, Koonin EV, Aravind L. Evolution and classification of P-loop kinases and related proteins. J Mol Biol. 2003; 333:781–815. [PubMed: 14568537]

Lo YH, Tsai KL, Sun YJ, Chen WT, Huang CY, Hsiao CD. The crystal structure of a replicative hexameric helicase DnaC and its complex with single-stranded DNA. Nucleic Acids Res. 2009; 37:804–814. [PubMed: 19074952]

Lu YB, Ratnakar PVAL, Mohanty BK, Bastia D. Direct physical interaction between DnaG primase and DnaB helicase of Escherichia coli is necessary for optimal synthesis of primer RNA. Proceedings of the National Academy of Sciences of the United States of America. 1996; 93:12902–12907. [PubMed: 8917517]

Lyubimov AY, Strycharska M, Berger JM. The nuts and bolts of ring-translocase structure and mechanism. Curr Opin Struct Biol. 2011; 21:240–248. [PubMed: 21282052]

Makowska-Grzyska M, Kaguni JM. Primase directs the release of DnaC from DnaB. Mol Cell. 2010; 37:90–101. [PubMed: 20129058]

Martinez-Jimenez MI, Mesa P, Alonso JC. Bacillus subtilis tau subunit of DNA polymerase III interacts with bacteriophage SPP1 replicative DNA helicase G40P. Nucleic Acids Res. 2002; 30:5056–5064. [PubMed: 12466528]

Mitkova AV, Khopde SM, Biswas SB. Mechanism and stoichiometry of interaction of DnaG primase with DnaB helicase of Escherichia coli in RNA primer synthesis. J Biol Chem. 2003; 278:52253–52261. [PubMed: 14557266]

Nakayama N, Arai N, Kaziro Y, Arai K. Structural and functional studies of the dnaB protein using limited proteolysis. Characterization of domains for DNA-dependent ATP hydrolysis and for protein association in the primosome. J Biol Chem. 1984; 259:88–96. [PubMed: 6323419]

Nitharwal RG, Verma V, Subbarao N, Dasgupta S, Choudhury NR, Dhar SK. DNA binding activity of Helicobacter pylori DnaB helicase: the role of the N-terminal domain in modulating DNA binding activities. FEBS J. 2012; 279:234–250. [PubMed: 22074440]

Oakley AJ, Loscha KV, Schaeffer PM, Liepinsh E, Pintacuda G, Wilce MC, Otting G, Dixon NE. Crystal and solution structures of the helicase-binding domain of Escherichia coli primase. J Biol Chem. 2005; 280:11495–11504. [PubMed: 15649896]

Pomerantz RT, O'Donnell M. Replisome mechanics: insights into a twin DNA polymerase machine. Trends Microbiol. 2007; 15:156–164. [PubMed: 17350265]

Remus D, Diffley JF. Eukaryotic DNA replication control: lock and load, then fire. Curr Opin Cell Biol. 2009; 21:771–777. [PubMed: 19767190]

San Martin C, Radermacher M, Wolpensinger B, Engel A, Miles CS, Dixon NE, Carazo JM. Three-dimensional reconstructions from cryoelectron microscopy images reveal an intimate complex between helicase DnaB and its loading partner DnaC. Structure. 1998; 6:501–509. [PubMed: 9562559]

San Martin MC, Stamford NP, Dammerova N, Dixon NE, Carazo JM. A structural model for the Escherichia coli DnaB helicase based on electron microscopy data. J Struct Biol. 1995; 114:167–176. [PubMed: 7662485]

Seitz H, Weigel C, Messer W. The interaction domains of the DnaA and DnaB replication proteins of Escherichia coli. Mol Microbiol. 2000; 37:1270–1279. [PubMed: 10972842]

Singleton MR, Dillingham MS, Wigley DB. Structure and mechanism of helicases and nucleic acid translocases. Annu Rev Biochem. 2007; 76:23–50. [PubMed: 17506634]

Singleton MR, Sawaya MR, Ellenberger T, Wigley DB. Crystal structure of T7 gene 4 ring helicase indicates a mechanism for sequential hydrolysis of nucleotides. Cell. 2000; 101:589–600. [PubMed: 10892646]

Syson K, Thirlway J, Hounslow AM, Soultanas P, Waltho JP. Solution structure of the helicase-interaction domain of the primase DnaG: a model for helicase activation. Structure. 2005; 13:609–616. [PubMed: 15837199]

Tamura JK, Gellert M. Characterization of the Atp Binding-Site on Escherichia-Coli DNA Gyrase - Affinity Labeling of Lys-103 and Lys-110 of the B-Subunit by Pyridoxal 5'-Diphospho-5'-Adenosine. Journal of Biological Chemistry. 1990; 265:21342–21349. [PubMed: 2174443]

Thomsen ND, Berger JM. Running in reverse: the structural basis for translocation polarity in hexameric helicases. Cell. 2009; 139:523–534. [PubMed: 19879839]

Tougu K, Marians KJ. The interaction between helicase and primase sets the replication fork clock. J Biol Chem. 1996; 271:21398–21405. [PubMed: 8702921]

Wahle E, Lasken RS, Kornberg A. The dnaB-dnaC replication protein complex of Escherichia coli. II. Role of the complex in mobilizing dnaB functions. J Biol Chem. 1989; 264:2469–2475. [PubMed: 2536713]

Wang G, Klein MG, Tokonzaba E, Zhang Y, Holden LG, Chen XS. The structure of a DnaB-family replicative helicase and its interactions with primase. Nat Struct Mol Biol. 2008; 15:94–100. [PubMed: 18157148]

Wang J. Nucleotide-dependent domain motions within rings of the RecA/AAA(+) superfamily. J Struct Biol. 2004; 148:259–267. [PubMed: 15522774]

Weigelt J, Brown SE, Miles CS, Dixon NE, Otting G. NMR structure of the N-terminal domain of E. coli DnaB helicase: implications for structure rearrangements in the helicase hexamer. Structure. 1999; 7:681–690. [PubMed: 10404597]

Xie Y, He ZG. Characterization of physical interaction between replication initiator protein DnaA and replicative helicase from Mycobacterium tuberculosis H37Rv. Biochemistry (Mosc). 2009; 74:1320–1327. [PubMed: 19961412]

Yang S, Yu X, VanLoock MS, Jezewska MJ, Bujalowski W, Egelman EH. Flexibility of the rings: structural asymmetry in the DnaB hexameric helicase. J Mol Biol. 2002; 321:839–849. [PubMed: 12206765]

Yu X, Jezewska MJ, Bujalowski W, Egelman EH. The hexameric E. coli DnaB helicase can exist in different Quaternary states. J Mol Biol. 1996; 259:7–14. [PubMed: 8648650]

Highlights

- DnaB helicases rely on a conserved N-terminal collar domain for assembly and function
- ATP binding by DnaB's motor domains switches the collar into a new conformation
- Collar conformation controls the ATPase and translocation properties of DnaB
- Partner proteins can read out collar state to regulate and respond to DnaB status

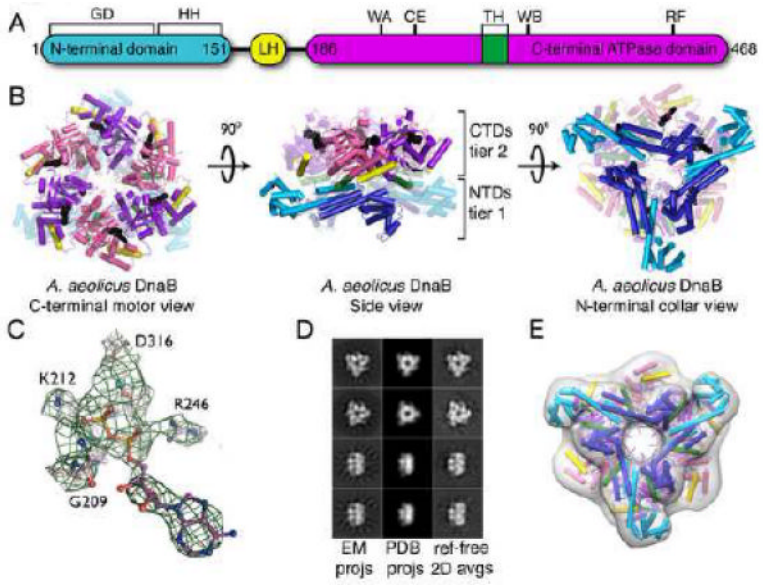

Figure 1. *Aa*DnaB structure

A) Domain organization. Specific regions discussed in the text are labeled. B) Cartoon representation of hexameric *Aa*DnaB, shown in three views. Coloring of structural elements as per panel A. C) Composite-omit electron density (at 4σ) of ADP•Mg^{2+} and nearby residues. D) Reference-free 2D class averages of *Aa*DnaB compared to forward re-projections of both the 3D EM model and the crystal structure. E) Fitting of the *Aa*DnaB crystal structure into the 3D EM reconstruction.

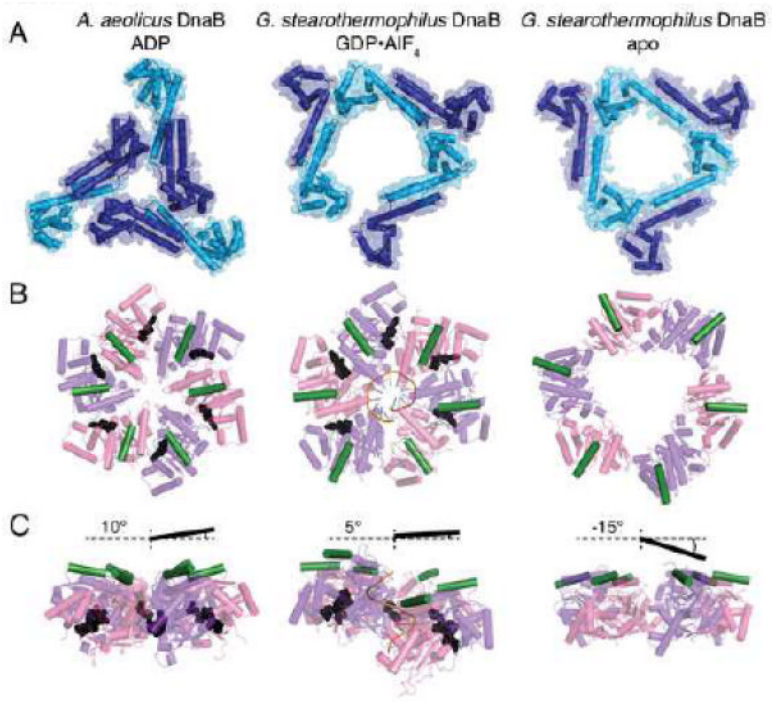

Figure 2. The DnaB N-terminal collar is a conformational switch

N-terminal collar (A), and top (B) and side (C) views of the C-terminal motor ring for ADP-bound *Aa*DnaB (left), DNA- and GDP•AlF_X-bound *Gst*DnaB (middle, PDB ID 4ESV), and apo *Gst*DnaB (right, PDB ID 2R6A). Subunits are alternatingly shaded light and dark to emphasize the transitions between N-terminal domain homodimers. The angle of the transducer helix (green) orientation relative to the plane of the ring is shown above the side views of the motor domain (C).

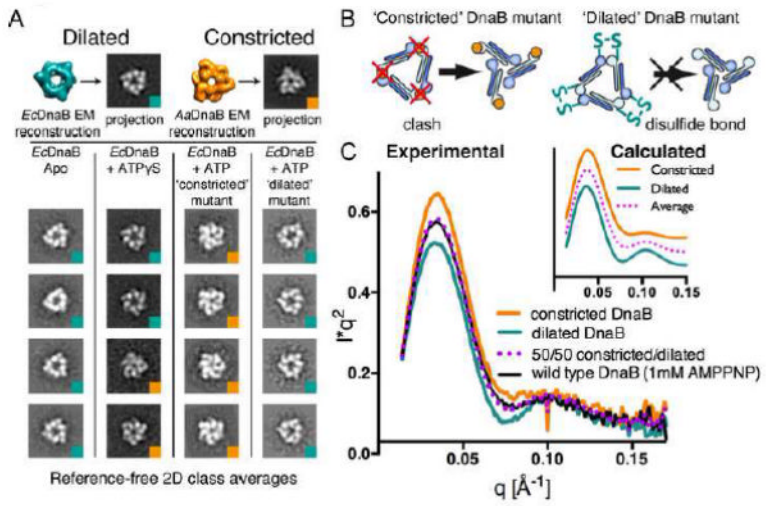

Figure 3. Nucleotide promotes DnaB constriction

A) Reference-free 2D class averages of wild type *Ec*DnaB and two collar mutants with different nucleotides. Dilated *Ec*DnaB and constricted *Aa*DnaB EM models are shown at top for comparison. B) Schematic design of the N-terminal collar mutants; green "S-S" connectors represent disulfide bonds formed in the dilated state, while red "X's" correspond to amino acids in *Ec*DnaB that, when mutated, prevent formation of the dilated state. C) Experimental SAXS curves of *Ec*DnaB with 1mM AMPPNP (black), constricted *Ec*DnaB (orange), dilated *Ec*DnaB (green) and average between the two states (pink dotted line). Inset: theoretical scattering curves of dilated (green) and constricted (orange) DnaB rings, as well as the average of the two models (pink dash) – curves are offset for clarity.

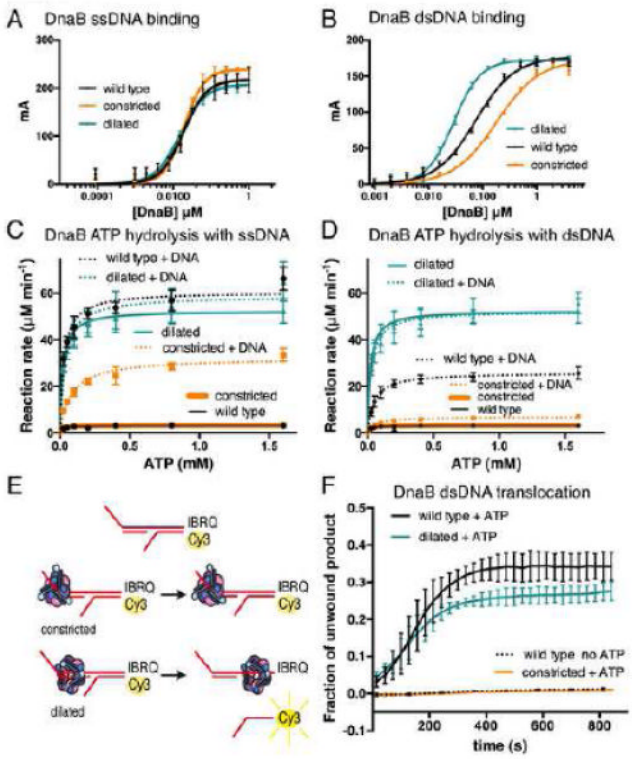

Figure 4. The N-terminal collar conformation affects helicase interactions with DNA and ATPase rate

Panels (A) and (B) correspond to single-stranded DNA binding and duplex DNA binding by wild type (black), constricted (orange) and dilated (green) *Ec*DnaB, respectively, as measured by fluorescence anisotropy (mA – milli-anisotropy units). Panels (C) and (D) correspond to ATP hydrolysis in the presence of single-stranded DNA (dotted lines in panel C) and duplex DNA (dotted lines in panel D), respectively. E) Schematic outline of experiment assaying translocation along duplex DNA. F) Kinetic data showing the ability of wild type (black), constricted (orange) and dilated (green) *Ec*DnaB to translocate along duplex DNA.

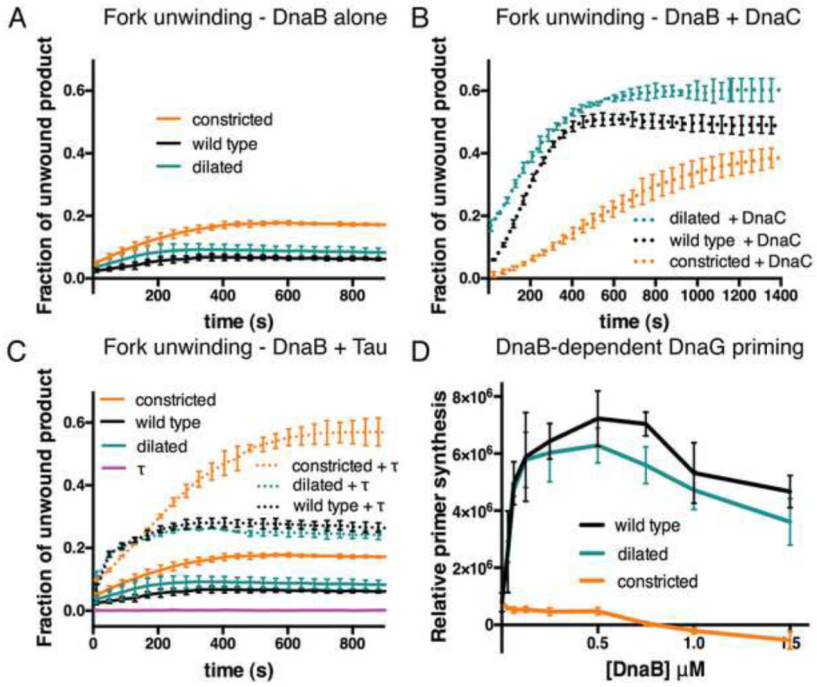

Figure 5. DNA unwinding and DnaB-partner interactions are influenced by collar state

A) Basal unwinding levels of a short forked substrate by wild type *Ec*DnaB (black) and both constricted (orange) and dilated (green) DnaB mutants. B) DnaC-dependent activation of DNA unwinding by DnaB and both constricted and dilated DnaB mutants. DnaC preferentially activates DNA unwinding by DnaB helicases that can access a dilated collar conformation. C) Effect of τ on DNA unwinding by DnaB. τ preferentially activates DNA unwinding by DnaB when the helicase favors a constricted collar conformation. D) Primer synthesis by DnaG in the presence of wild type and collar mutants of *Ec*DnaB. Only helicases that can adopt a dilated collar stimulate primer synthesis.

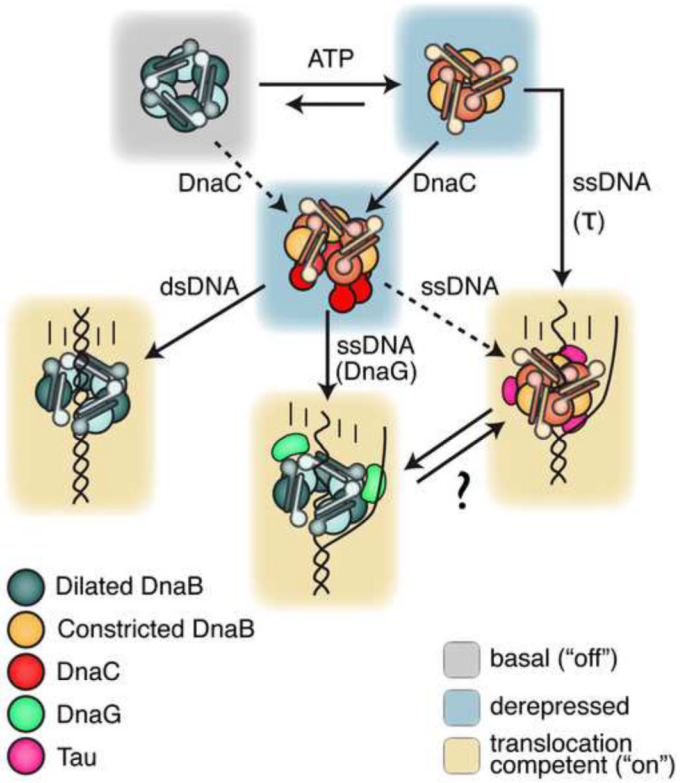

Figure 6. Potential roles for conformational switching in the N-terminal collar as a means to regulate DnaB function

Schematic illustrating how DnaB could use different collar states to switch from basal, low-activity states into translocation-competent forms, and how both substrates and partner proteins preferentially interact with and/or help control collar transitions and ring opening. Dashed lines represent less favored transitions based on data presented here and from the literature.

TABLE 1

SUMMARY OF X-RAY PARAMETERS

Data Collection	
Wavelength (Å)	1.1
Resolution range (Å)	69.2 - 3.3 (3.5 - 3.3)
Space group	$I2_13$
Unit cell (a, b, c)	195-7 195-7 195-7
(α, β, γ)	90.0° 90.0° 90.0°
Total reflections	101479(12875)
Unique reflections	18608 (1611)
Multiplicity	5.5 (5.2)
Completeness (%)	98.4 (85.1)
Mean I/σ (I)	8.9 (2.3)
Wilson B-factor	92.7
R_{merge} [a]	0.116 (0.554)
R_{pim} [b]	0.053 (0.256)
Refinement	
R_{work} [c]	0.236 (0.349)
R_{free} [d]	0.275 (0.373)
Number of atoms	6804
macromolecules	6732
ligands	57
water	15
Protein residues	839
RMS(bonds)	0.006
RMS(angles)	1.16
Ramachandran favored (%)	97.0
Ramachandran allowed (%)	2.76
Ramachandran outliers (%)	0.24
Average B-factor	100.5
macromolecules	100.7
ligands	85.3
solvent	49.3

[a] $R_{merge}=\sum_{hkl}\sum_i|I_i(hkl)-\overline{I(hkl)}|/\sum_{hkl}\sum_i I_i(hkl)$

[b] $R_{pim}=\sum_{hkl}\left(\frac{1}{N-1}\right)^{1/2}\sum_i|I_i(hkl)-\overline{I(hkl)}|/\sum_{hkl}\sum_i I_i(hkl)$

[c] $R_{work}=\sum||F_0|-|F_c||/\sum|F_0|$

[d] R_{free} was calculated using 5% of data omitted from refinement